

## Tuning Hydrated Nanoceria Surfaces: Experimental/Theoretical Investigations of Ion Exchange and Implications in Organic and Inorganic Interactions

Abhilash Vincent,<sup>†</sup> Talgat M. Inerbaev,<sup>‡</sup> Suresh Babu,<sup>†</sup> Ajay S. Karakoti,<sup>†</sup> William T. Self,<sup>§</sup> Artém E. Masunov,<sup>\*,†,||,⊥</sup> and Sudipta Seal<sup>\*,†,‡</sup>

<sup>†</sup>Advanced Materials Processing and Analysis Center, Department of Mechanical, Materials and Aerospace Engineering, University of Central Florida, Orlando, Florida 32816, <sup>‡</sup>Nanoscience Technology Center, University of Central Florida, Orlando, Florida 32826, <sup>§</sup>Department of Molecular Biology and Microbiology, Burnett School of Biomedical Sciences, University of Central Florida, Orlando, Florida 32816, <sup>||</sup>Department of Chemistry, University of Central Florida, Orlando, Florida 32816, and <sup>⊥</sup>Department of Physics, University of Central Florida, Orlando, Florida 32816

Received November 11, 2009. Revised Manuscript Received January 19, 2010

Long-term stability and surface properties of colloidal nanoparticles have significance in many applications. Here, surface charge modified hydrated cerium oxide nanoparticles (CNPs, also known as nanoceria) are synthesized, and their dynamic ion exchange interactions with the surrounding medium are investigated in detail. Time-dependent zeta ( $\zeta$ ) potential (ZP) variations of CNPs are demonstrated as a useful characteristic for optimizing their surface properties. The surface charge reversal of CNPs observed with respect to time, concentration, temperature, and doping is correlated to the surface modification of CNPs in aqueous solution and the ion exchange reaction between the surface protons ( $H^+$ ) and the neighboring hydroxyls ions ( $OH^-$ ). Using density functional theory (DFT) calculations, we have demonstrated that the adsorption of  $H^+$  ions on the CNP surface is kinetically more favorable while the adsorption of  $OH^-$  ions on CNPs is thermodynamically more favorable. The importance of selecting CNPs with appropriate surface charges and the implications of dynamic surface charge variations are exemplified with applications in microelectronics and biomedical.

### Introduction

Nanoparticles (NPs) of size less than 100 nm exhibit remarkably different properties from their bulk counterparts displaying a potential for their use in various application, ranging from catalysis,<sup>1</sup> photonics,<sup>2</sup> optoelectronics,<sup>3</sup> biological labeling,<sup>4</sup> and targeted drug delivery.<sup>5</sup> The homogenization, dispersion, and stabilization of NPs in suspension are of primary importance for their high performance in many applications.<sup>6</sup> Since the surface energy of NPs is significantly higher than that of larger particles,<sup>7</sup> nanoparticle (NP) sols are extremely sensitive to the changes in their physicochemical environment such as pH, ionic strength, temperature, and concentration, which in turn influences their agglomeration in suspensions.<sup>8</sup> A stable colloidal NP suspension can be obtained by balancing the attractive van der Waals forces acting between the NPs against the repulsive Columbic forces induced by the surface adsorbed species. Such suspensions

are often formed by providing steric or electrostatic stability by adding chemical additives to adjust the suspension properties such as viscosity, ionic strength, and pH<sup>9</sup> or by surface functionalization of the NPs themselves.<sup>10</sup> However, addition of chemicals may add more complexity to the system and may be undesirable. For example, pure NP suspensions are required for targeted drug delivery and cellular uptake,<sup>5,11</sup> where the interactions between NPs and biomacromolecules, cells, or living tissues determine the toxicity.<sup>8</sup> Surface charge modification of NPs through acidic or basic buffer treatment and subsequent dispersion in water is an attractive route to form stable suspension suitable for variety of applications.<sup>11</sup>

Cerium is a rare earth element of the lanthanide series. The oxide form of cerium ( $CeO_2$ ) has been widely used for glass polishing.<sup>12</sup> Currently, CNPs have been used in catalytic conversion,<sup>13</sup> solid oxide fuel cell,<sup>14</sup> and oxygen gas sensor.<sup>15</sup> Recent advancements in bionanomaterials research have proven the superoxide dismutase (SOD) mimetic radical scavenging activity

\*To whom correspondence should be addressed: e-mail amasunov@mail.ucf.edu, Tel (407) 882-2840, Fax 407 882-2819 (A.E.M.); e-mail sseal@mail.ucf.edu, Tel (407) 823-5277, Fax (407) 882-1462 (S.S.).

(1) Lewis, L. N. *Chem. Rev.* **2002**, 93(8), 2693.

(2) Maier, S. A.; Brongersma, M. L.; Kik, P. G.; Meltzer, S.; Requicha, A. A. G.; Atwater, H. A. *Adv. Mater.* **2001**, 13(19), 1501.

(3) Kamat, P. V. *J. Phys. Chem. B* **2002**, 106(32), 7729.

(4) Nicewarner-Peña, S. R.; Freeman, R. G.; Reiss, B. D.; He, L.; Peña, D. J.; Walton, I. D.; Cromer, R.; Keating, C. D.; Natan, M. J. *Science* **2001**, 294(5540), 137.

(5) Vincent, A.; Babu, S.; Heckert, E.; Dowding, J.; Hirst, S. M.; Inerbaev, T. M.; Self, W. T.; Reilly, C. M.; Masunov, A. E.; Rahman, T. S.; Seal, S. *ACS Nano* **2009**, 3(5), 1203.

(6) Karimian, H.; Babaloo, A. A. *J. Eur. Ceram. Soc.* **2007**, 27(1), 19.

(7) Artel, C.; Schmid, H.-J.; Peukert, W. *J. Aerosol Sci.* **2005**, 36(2), 147.

(8) Qi, L.; Sehgal, A.; Castaing, J.-C.; Chapel, J.-P.; Fresnais, J.; Berret, J.-F.; Cousin, F. *ACS Nano* **2008**, 2(5), 879.

(9) Brant, J.; Lecoanet, H.; Hotze, M.; Wiesner, M. *Environ. Sci. Technol.* **2005**, 39(17), 6343.

(10) Tang, E.; Cheng, G.; Ma, X.; Pang, X.; Zhao, Q. *Appl. Surf. Sci.* **2006**, 252(14), 5227.

(11) Patil, S.; Sandberg, A.; Heckert, E.; Self, W.; Seal, S. *Biomaterials* **2007**, 28(31), 4600.

(12) Duncan, L. K. *Glass Ind.* **1960**, 41, 412.

(13) Croy, J.; Mostafa, S.; Liu, J.; Sohn, Y.; Heinrich, H.; Cuenya, B. *Catal. Lett.* **2007**, 119(3), 209.

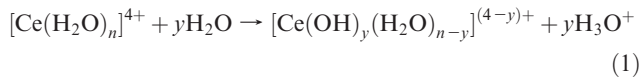
(14) Eguchi, K.; Setoguchi, T.; Inoue, T.; Arai, H. *Solid State Ionics* **1992**, 52(1–3), 165.

(15) Jasinski, P.; Suzuki, T.; Anderson, H. U., *Sens. Actuators, B* **2003**, 95(1–3), 73.

of CNPs in protecting cells against oxidative stress.<sup>16–18</sup> The unique property of CNPs, which makes them suitable for potential applications, originates from the increased concentration of Ce<sup>3+</sup> ions with the reduction in the size of the CNPs and their relative ease to undergo reversible redox reaction between Ce<sup>3+</sup> and Ce<sup>4+</sup> states (due to the presence of oxygen vacancy).<sup>19</sup> Because of their biocompatibility, small size, and cell membrane permeation capabilities, CNPs conjugated with ligand proteins have been identified as potential drug carriers that can target and release drugs to cancerous cells. Our earlier studies have shown that the efficiency of surface modified CNPs to successfully target cancer cells and undergo internalization mainly depends on the stability of the CNP–ligand binding which is often influenced by their surface chemistry.<sup>5</sup> The nature and long-term stability of the modified surface charges on CNPs and their behavior under different physiological conditions are relatively unknown, and a detailed study is necessary to explore the physicochemical changes taking place on the CNP surface under these conditions. Similarly, for applications such as in Chemical Mechanical Planarization (CMP), the interaction between CNP and silica surface in the slurry can be greatly influenced by the changes in the surface charges of CNPs.<sup>20</sup> Hence, a molecular level understanding of surface reactions occurring with time, temperature, concentration of CNPs, and associated changes in surface charges is essential to develop applications where long-term surface stability of NPs is highly desirable. Herein we report the surface charge variations of CNPs measured in terms of their ZPs as a function of aging time, dispersion temperature, concentration, CNP annealing temperature, and doping and their influence in targeted drug delivery and chemical mechanical polishing.

## Materials and Methods

**Synthesis of CNPs.** Cerium nitrate hexahydrate (Ce(NO<sub>3</sub>)<sub>3</sub>·6H<sub>2</sub>O, 99%, Aldrich) was used as a precursor for synthesizing CNPs.<sup>21</sup> To 0.1 M aqueous cerium nitrate solution (500 mL), 1.0 N ammonium hydroxide (NH<sub>4</sub>OH, Alfa Aesar) solution was added to maintain the pH at 9 and stirred for 4 h. Deionized water (18.0 mΩ) purified in a Barnstead NANOpure Diamond system was used for all the experiments. The resultant solution was stirred and allowed to settle overnight. The precipitates were washed with water multiple times to remove any weakly adhered ions on the surface and dried at 100 °C to obtain the CNPs. It is reported earlier<sup>22</sup> that the precipitation of Ce(NO<sub>3</sub>)<sub>3</sub>·6H<sub>2</sub>O precursor solution requires oxidation of Ce<sup>3+</sup> to Ce<sup>4+</sup> ions in solution. The addition of excess NH<sub>4</sub>OH to the Ce<sup>3+</sup> precursor solution leads to the oxidation of Ce<sup>3+</sup> to Ce<sup>4+</sup> ions. Because of their low basicity and higher ionic charge, Ce<sup>4+</sup> ions undergo strong hydration to form hydroxide complex.



This complex will undergo polymerization. In aqueous solution, due to its polar nature, H<sub>2</sub>O tends to take the excess

(16) Chen, J.; Patil, S.; Seal, S.; McGinnis, J. F. *Nat. Nanotechnol.* **2006**, 1(2), 142.

(17) Das, M.; Patil, S.; Bhargava, N.; Kang, J. F.; Riedel, L. M.; Seal, S.; Hickman, J. J. *Biomaterials* **2007**, 28(10), 1918.

(18) Tarnuzzer, R. W.; Colon, J.; Patil, S.; Seal, S. *Nano Lett.* **2005**, 5(12), 2573.

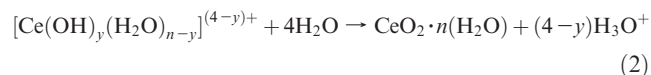
(19) Deshpande, S.; Patil, S.; V. N., T.; Kuchibhatla, S.; Seal, S. *App. Phys. Lett.* **2005**, 87(13), 133113.

(20) Suphantharida, P.; Osseo-Asare, K. *J. Electrochem. Soc.* **2004**, 151(10), G658.

(21) Babu, S.; Schulte, A.; Seal, S. *Appl. Phys. Lett.* **2008**, 92(12), 123112.

(22) Pei-Lin, C.; Chen, I.-W. *J. Am. Ceram. Soc.* **1993**, 76(6), 1577.

protons away from the hydroxide complex.



The precipitation of the hydrated CeO<sub>2</sub>·n(H<sub>2</sub>O) species leads to the formation of CNPs according to the dissolution precipitation mechanism. The precipitated particles were centrifuged and washed with deionized water multiple times to remove any impurities attached to the surface. Resultant NP powder was dried at 100 °C and was analyzed by both X-ray diffraction (Rigaku Model) and high-resolution transmission electron microscopy (Philips Tecnai operated at 300 keV).

**Tuning the Surface Charges of CNPs.** NPs tuned with positive or negative surface charge groups usually form strong electrostatic bonds with ligand molecules having oppositely charged groups. To study the stability of modified surface charges of CNPs, both positively and negatively charged CNPs were prepared by treating with different acidic and alkaline pH buffers in the range of pH 3–13. All these buffers were prepared by adding known amount of concentrated HCl or KOH (as necessary to adjust the pH) to 0.05 M KCl solution. This preparation ensured similar types of ions (H<sup>+</sup>, OH<sup>-</sup>, K<sup>+</sup>, and Cl<sup>-</sup>) in all buffers. The surface charges of CNPs were varied by treating 5 mg of the CNPs with 5 mL of pH buffer at a 1 mg/mL final concentration. The suspension was ultrasonicated for an hour and stirred using a magnetic stirrer for another 24 h followed by centrifuging and redispersing in deionized water at a concentration of 1 mM. The centrifuging and redispersion cycles were repeated until the pH of the CNP solution becomes neutral. The ZP value of the CNP solution was measured using Zetasizer (Nano-ZS) from Malvern Instruments. The instrument uses a combination of laser Doppler velocimetry (LDV) and phase analysis light scattering (PALS) in a technique called M3-PALS to measure the NP electrophoretic mobility. The details of this method can be found elsewhere.<sup>23</sup> The electrophoretic mobility ( $u_\zeta$ ) is then converted to ZP according to the Henry equation:<sup>24</sup>

$$u_\zeta = \frac{2\zeta\epsilon}{3\eta} f(\kappa a) \quad (3)$$

where  $\zeta$  is the ZP of the particles,  $\epsilon$  and  $\eta$  are respectively the dielectric constant and viscosity of the medium, and  $f(\kappa a)$  is the Henry's function.  $\kappa a$  is a measure of the ratio of the particle radius to electrical double layer thickness. The value of  $f(\kappa a)$  was chosen as 1.5 (Smoluchowski approximation) as the zeta potential measurements were conducted in aqueous medium. The original ZP values obtained were rounded to three significant figures and are represented as approximations.

**Time, Temperature, and Concentration Dependent Aging of CNPs.** Time, temperature, and concentration dependent ZP variations of CNPs were monitored at different intervals, and the effects of aging conditions on the ZPs of CNPs were investigated in detail. To study the influence of aging time on the ZPs of CNPs, solutions of both positively and negatively charged CNPs (obtained by acidic and alkaline buffer treatment) kept under normal atmospheric conditions (room temperature) were monitored for several months, and their respective ZP variations were plotted against aging time. The role of aging temperature on ZPs of CNPs was determined by heating the positively charged CNP in solution at different temperatures and recording their changes at each temperature. Similarly to study the concentration-dependent ZP variations, positively charged CNPs in solutions were diluted at different concentrations in the micromolar regime (concentrations of interest for cellular uptake studies), and their respective ZPs were reordered against their concentrations. In the

(23) Mezei, A.; Mészáros, R. *Langmuir* **2006**, 22(17), 7148.

(24) Henry, D. C. *Proc. R. Soc. London* **1931**, A133(821), 106.

temperature dependent study, the ZPs of CNPs were compared with that of doped, annealed, and micrometer ceria (purchased from Johnson Matthey) particles. Yttrium (Y) and ytterbium (Yb) were chosen to prepare doped CNPs as their ionic radii were respectively larger and smaller than that of pure cerium.

**AFM Force Spectroscopy Measurements.** Atomic force microscopy (AFM)-based single molecule force spectroscopy (SMFS)<sup>5,25–28</sup> has proven to be one of the most versatile techniques that can induce molecule level interactions on surfaces using functionalized probes and at the same time monitor these interaction forces in piconewton resolution. SMFS were carried out to study the interaction between transferrin (Tf) protein and CNPs, using Solver pro scanning probe microscopy (SPM) with a SMENA controller from NT-MDT, Moscow, Russia. We used Tf conjugated AFM probes (procedure for Tf-AFM probe conjugation is reported in our earlier publication<sup>5</sup>) with an average spring constant of 0.05 N/m and a tip curvature radius of ~10 nm for force measurements. Samples were prepared by drop coating CNPs on an atomically smooth silicon surface. The forces of interaction between Tf and CNPs were measured using SMFS on these samples by landing the probe tip on to the NP surface. Tf interacted strongly with the NP surface upon contact. The nature of the bonding was influenced by the surface charge and surface chemistry of the NPs. Following the landing, the tip was retracted from the surface. This lead to the stretching of Tf and subsequent bond breakage between Tf and NPs. Quantitative information regarding the elastic stretching behavior of protein and their interactions with the NP surface can be obtained from the force curve analysis. The laser deflection–piezo displacement data obtained from the SMFS experiments were then converted to force against displacement of the tip from the sample surface using the following equation

$$D(t) = z(t) - \delta(z)/S \quad (4)$$

where  $D(t)$  is the distance between the AFM probe and the surface in nm,  $z(t)$  is the piezostage displacement,  $\delta(z)$  is the cantilever deflection in nA, and  $S$  is the sensitivity of the cantilever determined by calculating the slope of the part of the force–displacement curve reflecting the bending of the cantilever obtained on silicon sample. The force  $F(z)$  is calculated by using the Hooke's law for a linear elastic spring (cantilever) as

$$F(z) = k_c \delta(z)/S \quad (5)$$

where  $k_c$  is the spring constant of the cantilever.

Similarly to study the interaction between silica surface and CNPs in CMP slurry, AFM-based force–displacement spectroscopy measurements were carried out using AFM probes attached with 600 nm diameter silica bead. The average spring constant of the cantilever was 4.5 N/m. The forces of interaction between silica bead and CNPs drop-coated on silicon were measured by lowering the probe tip close to the CNP surface and retracting it until the silica bead–CNP adhesion breaks. In both the cases, multiple force measurements were carried out at different locations on CNPs-coated silicon samples, and the corresponding force values were plotted in the form of histograms.

**Computational Details.** The DFT calculations presented here were carried out with the plane-wave-based Vienna *ab initio* simulation package (VASP).<sup>29,30</sup> The electronic ground state is

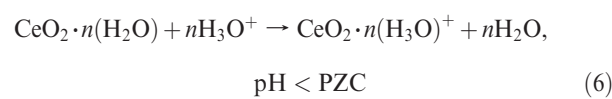
- (25) Oesterhelt, F.; Oesterhelt, D.; Pfeiffer, M.; Engel, A.; Gaub, H. E.; umlller, D. J. *Science* **2000**, 288(5463), 143.
- (26) Florin, E. L.; Moy, V. T.; Gaub, H. E. *Science* **1994**, 264(5157), 415.
- (27) Smith, B. L.; Schaffer, T. E.; Viani, M.; Thompson, J. B.; Frederick, N. A.; Kindt, J.; Belcher, A.; Stucky, G. D.; Morse, D. E.; Hansma, P. K. *Nature* **1999**, 399(6738), 761.
- (28) Oberhauser, A. F.; Marszalek, P. E.; Erickson, H. P.; Fernandez, J. M. *Nature* **1998**, 393(6681), 181.
- (29) Kresse, G.; Hafner, J. *Phys. Rev. B* **1993**, 47(1), 558.
- (30) Kresse, G.; Furthmüller, J. *Phys. Rev. B* **1996**, 54(16), 11169.

determined by using local density (LDA) approximation. We used the LDA+ $U$  version with local part described by Ceperley–Adler functional. On site Coulomb and exchange interaction are treated by a single effective parameter  $U_{\text{eff}} = U - J$ . Plane waves are included up to an energetic cutoff of 415 eV, the electronic wave functions were described using the projected augmented wave (PAW) method, and  $U_{\text{eff}} = 5$  eV.<sup>31</sup> These calculation parameters were recently employed for the investigation of ceria. It was shown that the LDA+ $U_{\text{eff}}$  approximation demonstrates better agreement for geometry with experiment than the GGA+ $U$  approach.<sup>32</sup> Energies of LDA+ $U_{\text{eff}}$  optimized structures were recalculated with Perdew–Burke–Ernzerhof (PBE) exchange–correlation functional using  $U_{\text{eff}} = 5.5$  eV.<sup>33</sup> Supercells were chosen with at least 10 Å between replicas to remove spurious periodic interactions while Coulomb interaction between periodic charged images is compensated according to the procedure reported earlier.<sup>34</sup>

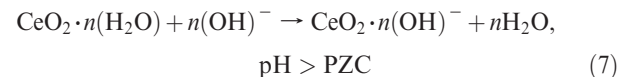
## Results and Discussion

**Time Dependent Surface Charge Modifications of Hydrated Nanoceria.** The structural and morphological properties of CNPs were determined by X-ray diffraction (XRD) and high-resolution transmission electron microscopy (HRTEM). From the HRTEM image, the mean particle size of CNPs was calculated to be ~8.2 ± 1 nm. Both XRD (Figure 1a) and selected area electron diffraction (SAED) (Figure 1b, inset) patterns of CNPs display the cerium oxide fluorite structure.

The surface charge of colloidal NPs is often addressed by measuring their ZP, an electrostatic potential that exists at the shear planes of the particles, related to both surface charge and the local environment of the particles. The pH at which the CNPs exhibit a ZP of magnitude close to zero (point of zero charge, PZC) is reported to be ~9.5.<sup>11</sup> The surface charge formulation on CNPs can be visualized as follows. When anhydrous cerium oxide is dispersed in water in the form of a colloidal suspension, it binds with H<sub>2</sub>O molecules to form hydrated CeO<sub>2</sub>. When the pH of the solution is less than the PZC of CNPs, hydrated CeO<sub>2</sub> absorbs a proton (H<sup>+</sup> ion) and forms a positive charged particle.<sup>35</sup>



Similarly, when the pH of the solution is greater than the PZC of CNPs, hydrated CeO<sub>2</sub> loses an H<sup>+</sup> ion from the bound H<sub>2</sub>O molecule and forms a negatively charged colloid particle.<sup>35</sup>



The interaction and the stability of the bond between hydrated CNPs and the H<sup>+</sup> or OH<sup>-</sup> ions governs the sign and magnitude of the ZPs of CNPs.

To determine the effect of aging time on the surface charges, ZPs of CNP solutions were monitored at regular intervals of time. Figure 2a shows the ZP of fresh CNPs (at a concentration of

- (31) Blöchl, P. E. *Phys. Rev. B* **1994**, 50(24), 17953.
- (32) Loschen, C.; Carrasco, J.; Neyman, K. M.; Illas, F. *Phys. Rev. B* **2007**, 75(3), 035115.
- (33) Castleton, C. W. M.; Kullgren, J.; Hermansson, K. *J. Chem. Phys.* **2007**, 127(24), 244704.
- (34) Makov, G.; Payne, M. C. *Phys. Rev. B* **1995**, 51(7), 4014.
- (35) Necula, B. S.; Apachitei, I.; Fratila-Apachitei, L. E.; Teodosiu, C.; Duszczuk, J. *J. Colloid Interface Sci.* **2007**, 314(2), 514.

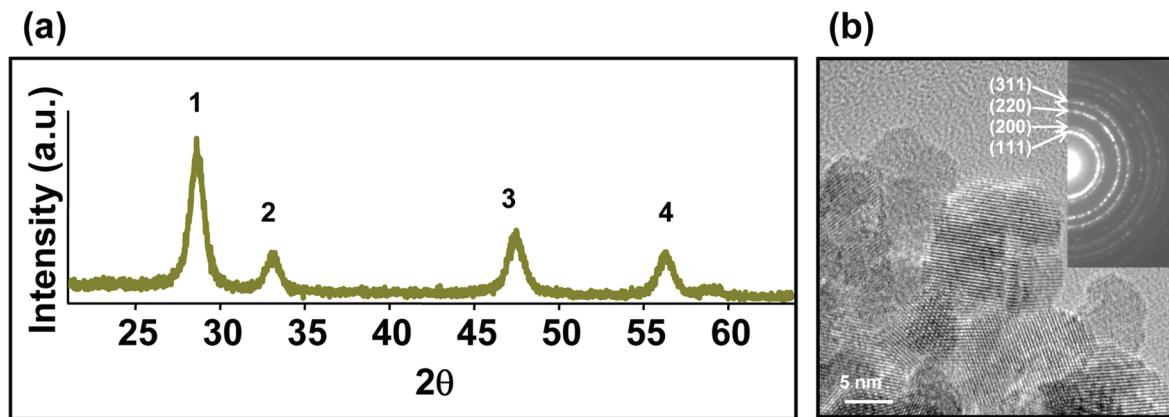


**Figure 1.** (a) XRD spectrum and (b) HRTEM image of fluorite structured CNPs. The peaks corresponding to positions 1, 2, 3, and 4 in the XRD spectrum represent the planes (111), (200), (220), and (311), respectively (JCPDS 81-0792). The inset in the HRTEM image shows the SAED pattern of CNPs. The CNP particle size is  $\sim 8.2 \pm 1$  nm.

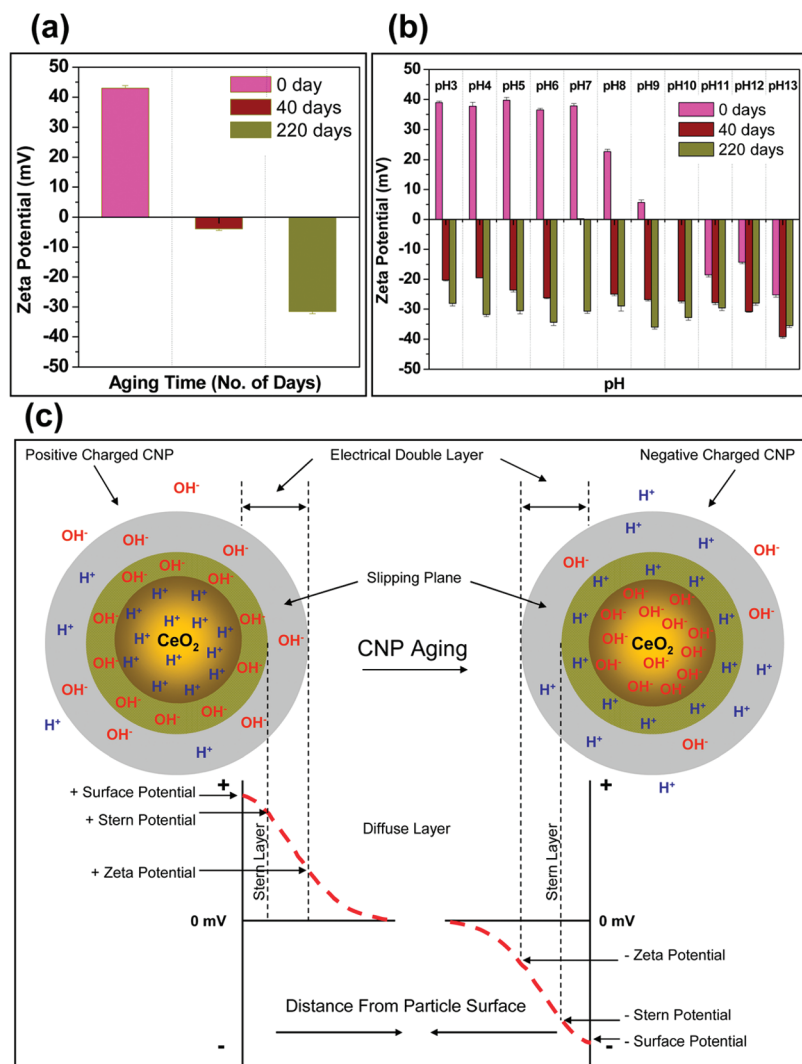


**Figure 2.** ZPs of freshly prepared CNPs (a) and CNPs treated with different pH buffers (b) aged at room temperature. Acid buffer treated CNPs resulted in positive ZP, and alkaline buffer treated CNPs resulted in negative ZP. Both untreated and buffer treated CNPs exhibited a time dependent shift of ZP from positive to negative charge. Negatively charged CNPs became more negative with time. (c) Schematic of potential distribution around positive and negative charged CNPs. Development of a net charge at the NP surface affects the distribution of  $\text{H}^+$  and  $\text{OH}^-$  ions in the surrounding interfacial region, resulting in an increased concentration of counterions (ions of charge opposite to that of the particle) close to the NP surface. During aging, positive charged CNPs display a tendency to replace their surface protons with  $\text{OH}^-$  counterions.

1 mM) aged at room temperature for 0, 40, and 220 days. Immediately after dispersing freshly prepared CNPs in water

(0 day), a high positive ZP of +43.0 mV was observed. This can be attributed to the formation of positively charged species

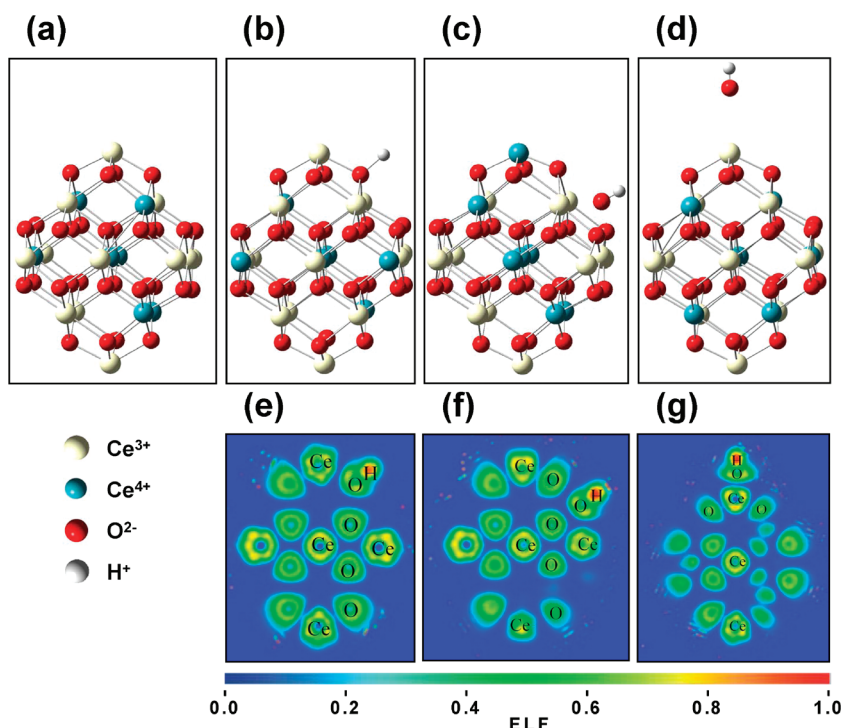


**Figure 3.** Atomic structure model of octahedral  $(\text{CeO}_{2-x})_{19}$  ( $x = 0.32$ ) NP obtained from the bulk cerium oxide by cutting through (111) planes with different molecular species adsorbed: (a) bare CNP, (b) CNP with  $\text{H}^+$  ion, (c) CNP with  $\text{OH}^-$  ion adsorbed on the facet, (d) CNP with  $\text{OH}^-$  ion adsorbed on the vertex.  $\text{Ce}^{3+}$ ,  $\text{Ce}^{4+}$ ,  $\text{O}^{2-}$ , and  $\text{H}^+$  ions are shown as light yellow, blue, red, and gray spheres, respectively. Projection of electron localization function (ELF) on different planes passing through CNP and adsorbed (e)  $\text{H}^+$  ion, (f)  $\text{OH}^-$  ion (facet), and (g)  $\text{OH}^-$  ion (vertex). Color codes blue (ELF = 0) and red (ELF = 1.0) represent full absence and full presence of electron pair in actual point of space. Adsorbed  $\text{H}^+$  ion forms a covalent bond with CNP while ionic bonding is observed between adsorbed  $\text{OH}^-$  ion and CNP.

( $\text{H}_3\text{O}^+$  ions) on CNP surface due to the increased dissociation of the  $\text{H}_2\text{O}$  molecules at CNP oxygen vacancies,<sup>36,37</sup> according to the eq 1. Also, CNPs exhibited a time dependent shift in ZP from positive to negative charges (+43.0, -3.90, and -31.5 mV at 0, 40, and 220 days, respectively). To further explore the surface charge dynamics, time dependent studies were carried out on both positive and negative charged CNPs formed via acidic or basic pH buffer treatment (CNPs were resuspended in deionized water after the buffer treatment). Figure 2b shows the ZPs of CNPs (1 mM) after treatment with a range of pH buffers (pH 3–14). CNPs treated with acidic pH buffers retained positive ZPs, while CNPs treated with alkaline pH buffers (pH 8–13) exhibited a gradual shift in ZP from positive to negative with increasing pH. The PZC of CNPs was observed at pH 10 (Figure 2b). After about 40 days, the ZP of all the positively charged CNPs changed to negative values, while the magnitude of negatively charged CNPs increased to higher negative values. The ZP measured in 220 days for all the pH-treated CNPs exhibited high negative ZPs values in the range of -26.0 to -36.0 mV. The time dependent shift in ZP from positive to negative values observed could be due to the replacement of the positively charged surface species from the NP surface ( $\text{H}^+$ ) with the negatively charged counterions ( $\text{OH}^-$  ions). Figure 2c shows the schematic of potential distribution around positive and negative charged CNP surface. It is clear that CNP's surface affects the distribution of  $\text{H}_3\text{O}^+$  and  $\text{OH}^-$  ions in the surrounding interfacial region, resulting in an increased concentration of counterions (ions of opposite charge) close to the CNP surface. Though both aging and pH buffer treatment resulted in

different surface charges, the size of CNPs remained the same in all these conditions. The HRTEM images of freshly prepared positively charged CNPs and aged negatively charged CNPs are shown in Supporting Information Figure S1.

**Proton and Hydroxyl Ion Interactions with Hydrated Nanoceria.** DFT simulation studies were conducted to understand the nature of molecular level interactions of  $\text{H}_3\text{O}^+$  and  $\text{OH}^-$  ion with CNPs dispersed in water. For simplicity, we modeled the CNP– $\text{H}_3\text{O}^+/\text{OH}^-$  ion interaction by considering a small CNP as shown in Figure 3a, which has a size of ~1 nm and  $\text{C}_{19}\text{O}_{32}$  stoichiometry. This is a minimal octahedral NP derived from a bulk cerium oxide fluorite lattice, exposing the most stable (111) facets in accordance with the HRTEM images of the CNPs shown in Figure 1b.

The bulk ionized water structures have been elucidated by previous *ab initio* molecular dynamics simulations,<sup>38</sup> which found that fast proton exchange processes lead to fluctuation between so-called Eigen ( $\text{H}_3\text{O}^+$ )<sup>39</sup> and Zundel ( $\text{H}_5\text{O}_2^+$ )<sup>40</sup> forms of hydronium. Modeling of  $\text{H}_3\text{O}^+$  ion interaction with CNP demonstrates that hydronium ion is unstable in the vicinity of CNP and decays to an  $\text{H}^+$  ion and a  $\text{H}_2\text{O}$  molecule. This  $\text{H}^+$  ion forms a covalent bond with CNP while the  $\text{H}_2\text{O}$  molecule gets adsorbed on to the CNP's surface by forming two hydrogen bonds. We performed CNP– $\text{H}_3\text{O}^+$  interaction simulations with the distance between CNP and hydronium oxygen fixed at 3 Å. Calculations predict that  $\text{H}_3\text{O}^+$  ion on the vicinity of CNP is highly unstable and will undergo barrierless dissociation reaction by proton transfer from

(36) Tabakova, T.; Bocuzzi, F.; Manzoli, M.; Sobczak, J. W.; Idakiev, V.; Andreeva, D. *Appl. Catal. A: Gen.* **2006**, 298, 127.

(37) Wang, X.; Rodriguez, J. A.; Hanson, J. C.; Gamarra, D.; Martínez-Arias, A.; Fernández-García, M. *J. Phys. Chem. B* **2006**, 110(1), 428.

(38) Tuckerman, M. E.; Marx, D.; Parrinello, M. *Nature* **2002**, 417(6892), 925.

(39) Eigen, M. *Angew. Chem., Int. Ed. Engl.* **1964**, 3(1), 1.

(40) Zundel, G. In *The Hydrogen Bond, Recent Developments in Theory and Experiments*; Schuster, P., Zundel, G., Sandorfy, C., Eds.; North-Holland: Amsterdam, 1976; Vol. II, p 683.

the H<sub>2</sub>O molecule to the CNP surface. This forms a metastable CNP–H<sup>+</sup> complex. However, after the equilibrium is established, the H<sup>+</sup> species on the CNP surface is replaced with OH<sup>-</sup> ion from the solution and forms the more stable CNP–OH<sup>-</sup> complex.

Figures 3b–d show the possible ways to conjugate H<sup>+</sup> and OH<sup>-</sup> ions on the CNP.<sup>41</sup> For H<sup>+</sup> ion there is only one possible way to be bonded to the oxygen atom on the NP surface, as shown in Figure 3b. There are two equilibrium positions for OH<sup>-</sup> ions: one on the facet position, in between the three oxygen atoms terminating the CNP's surface (Figure 3c), and the other position in the vertex of CNP near the cerium ion (Figure 3d). At the latter position OH<sup>-</sup> interacts significantly stronger with CNP as the main contribution toward binding interaction comes from the attractive Columbic interaction between cerium ion at vertex position and the neighboring OH<sup>-</sup> ion (Figure 3d). In the former case, interaction is partially screened by surface oxygen ions, and the value of the binding energy (BE) obtained between the OH<sup>-</sup> ion and facet cerium ion is smaller compared to that of vertex cerium ion. H<sup>+</sup> ion is covalently bonded to the CNP's surface oxygen while OH<sup>-</sup> ion is ionically bonded as seen from the electron localization function (ELF)<sup>42</sup> plots shown in Figures 3e–g.

The BE calculated for CNP–H<sup>+</sup> and CNP–OH<sup>-</sup> complexes as a function of the number of ligands (adsorbed species) are shown in Figure 4a. Here, the BE between CNP and  $n$  number of adsorbed X species is defined as

$$\text{BE} = [E(\text{CNP}) + nE(\text{X}) - E(\text{CNP}-n\text{X})]/n \quad (8)$$

where  $E(\text{CNP})$ ,  $E(\text{X})$ , and  $E(\text{CNP}-n\text{X})$  are the ground state energies for CNP, X species, and CNP with adsorbed X species, respectively.

As seen from Figure 4a, OH<sup>-</sup> ions interact with CNP significantly stronger than H<sup>+</sup> ions. This interaction is attractive, and its magnitude decreases with the number of additional OH<sup>-</sup> ions adsorbed by CNP. Among the two different equilibrium positions for OH<sup>-</sup> ions, the vertex position is found to be the more stable than facet position. Adsorption of OH<sup>-</sup> ions to these sites leads to a slight decrease in the BE values from 1.47 eV for one adsorbed OH<sup>-</sup> ion to 1.12 eV for six adsorbed OH<sup>-</sup> ion species. In the case of CNPs with a facet adsorbed OH<sup>-</sup> ion, the BE profile display a steady decreases from 1.31 to 0.37 eV. At the same time, BE values of H<sup>+</sup> ions steadily decreases and becomes negative for  $n > 2$ , indicating that the interaction between protonated CNP and H<sup>+</sup> ions becomes repulsive, and no further attachment of H<sup>+</sup> ions is possible on a doubly protonated CNP of the size studied here.

Experimental results revealed ZP changes from positive to negative values with time while the theoretical results predict that the CNPs exhibits a favorable tendency to bond to OH<sup>-</sup> ions in solution. Such experimentally observed changes in the sign of ZP indicate that kinetics of proton–hydroxyl ion exchange on CNP surface play a major role in the ZP sign reversal. To explain such behavior, the potential energies of the elementary processes responsible for the rates of the ion adsorption and desorption were calculated. Potential energy profiles were evaluated for a number of configurations constructed by varying the distance between CNP and adsorbed species (reaction coordinates). Geometrical optimization was performed for each structure by fixing the distance between adsorbed species and CNP (relaxed scan).

(41) Loschen, C.; Bromley, S. T.; Neyman, K. M.; Illas, F. *J. Phys. Chem. C* **2007**, *111*(28), 10142.

(42) Silvi, B.; Savin, A. *Nature* **1994**, *371*(6499), 683.

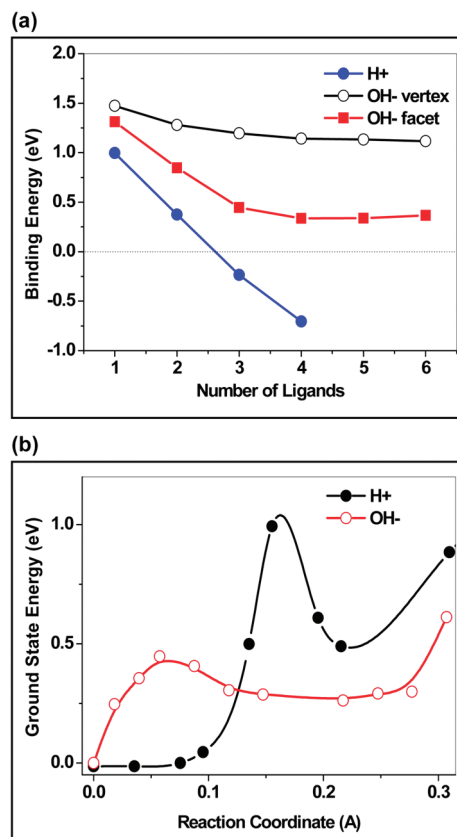


**Figure 4.** (a) Binding energies per adsorbed specie of OH<sup>-</sup> and H<sup>+</sup> ions with CNPs as a function of number of ions on the NP's surface. The BE calculations predict that Ce<sub>19</sub>O<sub>32</sub> NP is able to adsorb maximum two H<sup>+</sup> ions (positive ZP) while its ability for OH<sup>-</sup> adsorption is much higher. Adsorption of OH<sup>-</sup> ion on CNP's vertex and facets is considered. Larger BE values were observed for the interaction of OH<sup>-</sup> ion with Ce<sup>3+</sup> ion placed on the vertex of CNP. (b) The ground state energy profile for OH<sup>-</sup> and H<sup>+</sup> ions as a function of their distance from the equilibrium position on the CNP's facet that defines the zero point of energy. CNP with adsorbed OH<sup>-</sup> ion is more energetically favorable since, its BE is about 0.31 eV larger than the corresponding value for H<sup>+</sup> ion adsorption.

The obtained results are presented in Figure 4b. The CNP–H<sup>+</sup> NP is formed during the barrierless decay of Eigen cation in the vicinity of CNP as described above. The removal of H<sup>+</sup> ion from CNP proceeds through the breaking of the covalent bond between CNP and H<sup>+</sup>, which requires the overcoming of the energy barrier. Subsequently, the OH<sup>-</sup> ions have to overcome another energy barrier to form coordination bond with CNP surface and to reach the most stable low-energy state. This energy barrier originates from the redistribution of f-electron density in the CNP during the approach of OH<sup>-</sup> ion from the large distance to the equilibrium position on the CNP surface. The redistribution of Ce<sup>3+</sup> and Ce<sup>4+</sup> ions in CNPs is shown in parts a and d of Figure 3, respectively.

These computational results can be summarized as follows. When CNPs are introduced into the aqueous solution, their surface is protonated through the fast, diffusion-controlled process (diffusion of protons from the solution to the CNP surface), resulting in the formation of kinetically favorable CNP–H<sup>+</sup> complexes. This is the possible reason for the initial positive ZP observed for freshly prepared CNPs dispersed in water. During the aging process, the OH<sup>-</sup> ions slowly overcome the potential barrier to association and occupy the thermodynamically

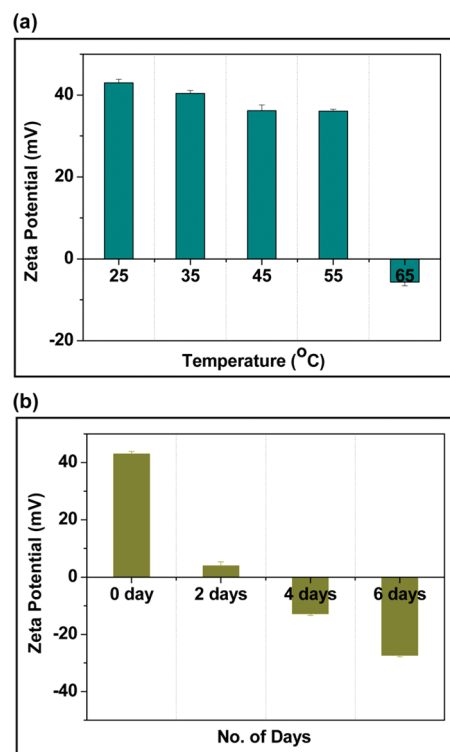


**Figure 5.** (a) ZPs of freshly prepared CNPs measured instantaneously at different temperatures within an equilibration time of 5 min. (b) ZPs of fresh CNPs heated at 65 °C and measured at 25 °C. ZP of CNPs gradually shifts from positive to negative values with time.

favorable positions by displacing the H<sup>+</sup> ions from the CNP surface. Thus, performed calculations explain the inversion in ZP observed during the aging of freshly prepared CNPs.

**Influence of Solution Temperature on the Surface Charge Modifications.** Since our experimental and theoretical observations indicate a kinetically controlled change in the CNP surface charge, we tested the effect of the parameters that can influence the kinetics, such as temperature and concentration. To determine the effect of the temperature on ZP, the CNP solutions (1 mM) were heated in situ from 25 to 65 °C, and their ZPs were measured at each temperature after reaching an equilibration time of 5 min (Figure 5a). Freshly prepared CNPs exhibit ZP values of +43.0, +40.4, +36.2, +36.1, and -5.68 mV at 25, 35, 45, 55, and 65 °C, respectively. Starting from 25 °C, the CNPs exhibited a decreasing trend in ZP (with marginal variations) until 55 °C. However, at 65 °C, CNPs exhibited an inversion in ZP sign from the positive to the negative value (-5.68 mV at 65 °C).

The nature of ZP changes observed while heating the CNP solution at different temperatures were similar to that observed in the case of CNP solutions aged for several days. Though heating at 65 °C resulted in negatively charged CNPs, cooling the solution back to room temperature displayed positive ZPs of lower magnitudes. Hence another set of experiment was initiated where the CNPs solution was maintained at 65 °C for several hours and the ZP was measured after cooling the suspension back to 25 °C. Figure 5b shows the ZP of CNP solution heated at 65 °C and measured at 25 °C. In a span of 6 days the ZP of the CNPs became stable and exhibited a negative ZP of -27.3 mV at room temperature (25 °C). Further heating of CNPs solution did not result in considerable ZP variations. These observations suggest that during the heat treatment accelerated dissociation of protons from CNP surface occurs, which is partially reversible. The

**Table 1. Calculated Charge Density ( $\sigma_d$ ) at Different Temperatures Using Dielectric Constant for Water ( $\epsilon_r$ ) and ZP**

T, °C	$\epsilon_r(\text{H}_2\text{O})$	$\epsilon (\times 10^{-10} \text{ F/m})$	$\zeta, \text{mV}$	$\sigma_d (\times 10^{-6} \text{ C/m}^2)$
25	78.4	6.95	43.0	1.10
35	74.6	6.64	40.4	0.973
45	71.3	6.33	36.2	0.820
55	68.2	6.03	36.1	0.784
65	65.1	5.74	-5.68	-0.111

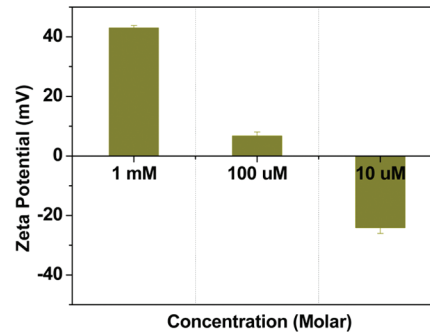


**Figure 6.** ZPs of fresh CNPs measured at 25 °C at different CNP concentrations. ZP of CNPs shifts from positive to negative with decrease in CNP concentration.

following association of CNPs with the hydroxyl ions from the solution proceeds at a slower rate.

The charge density of CNPs is related to their ZP as follows<sup>43</sup>

$$\sigma_d = (8\epsilon_0\epsilon_r RTC)^{1/2} \sinh\left(\frac{zF\zeta}{2RT}\right) \quad (9)$$

where R is the ideal gas constant, T is the absolute temperature, F is Faraday's constant, z is the valency of the ions,  $\sigma_d$  is the charge density of the NP,  $\epsilon_0$  is the electrical permittivity of a vacuum,  $\epsilon_r$  is the dielectric constant of the electrolyte assumed to be equal to that of water, and C is the concentration of the ions in the electrolyte in mol/L. H<sub>2</sub>O undergoes self-dissociation and form H<sub>3</sub>O<sup>+</sup> and OH<sup>-</sup> ions. For pure deionized water (pH 7) the concentrations of both the H<sub>3</sub>O<sup>+</sup> and OH<sup>-</sup> ions are equal to  $c = 10^{-7}$  mol/L. Table 1 displays the charge density calculated for CNPs in suspension heated to different temperatures. The charge density varies with the temperature in a manner similar to that of ZP.

**Concentration Dependent Surface Charge Modifications.** Most of the applications, including the biomedical ones, utilize the CNPs in nanomolar to micromolar concentrations.<sup>11</sup> The cell–CNP and protein–CNP interactions depend mainly on their surface charges. Hence, it is important to understand ZP behavior of CNPs at these concentrations. For this purpose, ZP of CNP solutions were tested at 1 mM, 100 μM, and 10 μM concentrations. Figure 6 shows ZPs of CNPs with respect to CNP concentrations measured at 25 °C. CNPs exhibited a ZP of +43.0, +6.70, and -24.1 mV at 1 mM, 100 μM, and 10 μM concentrations, respectively. A gradual shift in the ZP from positive to negative values was observed with decrease in molar concentration of the CNPs. Concentration dependent ZP variation was observed only below 1 mM concentration of CNPs, and the ZP remained at +43.0 mV for all concentrations above 1 mM. At 100 and 10 μM, the decrease in magnitude of positive ZP and its shift toward negative values indicates that the CNPs have a

(43) Zimmermann, R.; Dukhin, S.; Werner, C. *J. Phys. Chem. B* **2001**, 105(36), 8544.

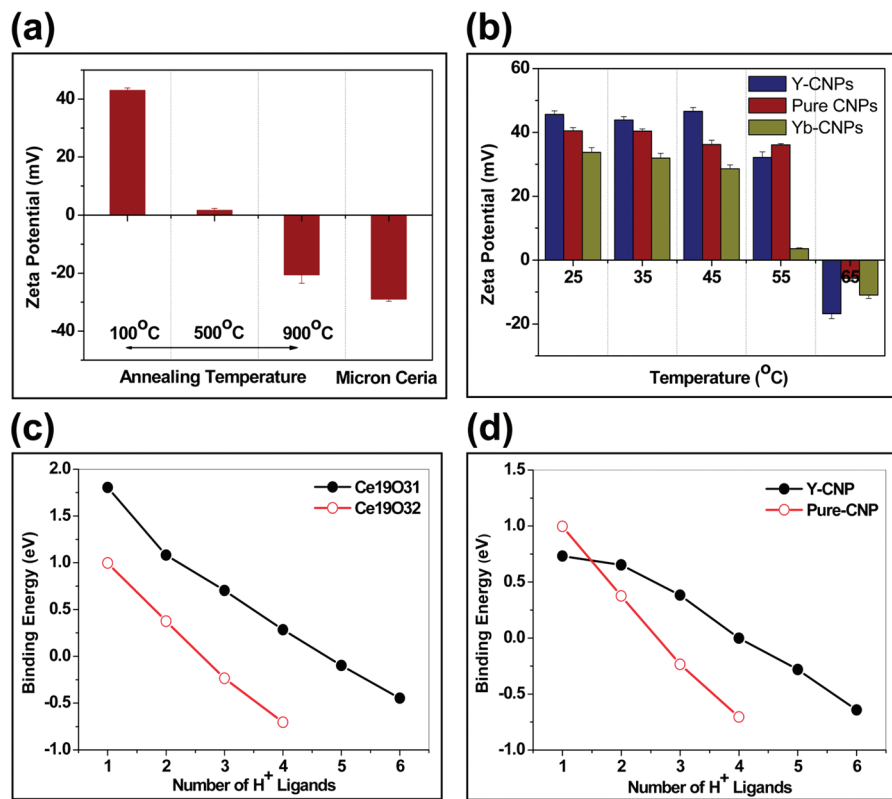


**Figure 7.** (a) ZPs of annealed CNPs and micrometer ceria and (b) ZPs of doped CNPs measured at different temperatures. ZP of doped CNPs changed from positive to negative with increase in measurement temperature. 100 °C annealed CNPs displayed positive ZP while high temperature annealed CNPs displayed negative ZP. Micron sized cerium oxide particles showed the highest negative ZP among all the samples. (c) Binding energy plot of H<sup>+</sup> ion with CNPs as a function of number of H<sup>+</sup> ions on the CNP surface. Plotted results correspond to perfect octahedral Ce<sub>19</sub>O<sub>32</sub> CNP (open circles) and CNP with one surface oxygen vacancy Ce<sub>19</sub>O<sub>31</sub> (filled circles). (d) Binding energy plot of H<sup>+</sup> ion with pure CNP (Ce<sub>19</sub>O<sub>32</sub>) and yttrium doped CNP (Ce<sub>15</sub>Y<sub>4</sub>O<sub>30</sub>) as a function of the number of H<sup>+</sup> ions on the CNP surface. The BE decreased in the order Y-CNP > pure-CNP, similar to the amount of oxygen vacancy concentration in these samples.

more pronounced tendency to associate with OH<sup>-</sup> ions at lower concentrations. When CNPs are diluted to micromolar concentrations, the rate of H<sub>2</sub>O dissociation and formation of H<sub>3</sub>O<sup>+</sup> and OH<sup>-</sup> ions could decrease. This leads to less interaction between CNPs and kinetically favorable H<sub>3</sub>O<sup>+</sup> ions and may effectively reduce the magnitude of positive charge on CNP surface (Figure 6). Since many of the drug/gene delivering ligands such as transferrin<sup>5</sup> and folic acid<sup>44</sup> exhibit negative ZP at physiological pH, the concentration dependent ZP changes indicates that it is essential to treat freshly prepared positively charged CNPs with ligand molecules at concentration above 1 mM for achieving better CNP–ligand conjugation and then dilute the resultant solution to the concentration of interest. Treating CNPs with ligand molecules directly at micromolar and nanomolar concentrations may lead to poor ligand adsorption due to the Coulombic repulsion between the ligands and negatively charged CNPs.

**Role of Oxygen Vacancy Defects on the Surface Charge Tunability.** The CNPs attracted great interest recently for various catalytic applications due to their ability to easily absorb and release oxygen. This oxygen storage capacity is a result of the oxygen vacancy formation in the CeO<sub>2</sub> lattice.<sup>45</sup> In the earlier sections, we have discussed the role of external material parameters such as aging time, solution temperature, and solution concentration on the ZPs of CNPs. To determine the effect of intrinsic material properties such as oxygen vacancies on ZP

values, CNPs were annealed at high temperature (100, 500, and 900 °C) in air atmosphere for 2 h to decrease the oxygen vacancy concentration. Annealing CNPs at high temperature in the air is expected to result in faster oxygen diffusion and subsequent annihilation of oxygen vacancies.<sup>46</sup> Following this annealing, the ZP of CNPs (1 mM) were measured, and the results are presented in Figure 7a. The CNPs annealed at 500 °C exhibit a low positive ZP value of +1.65 mV as compared to those annealed at 100 °C (+43.0 mV). The CNPs annealed at 900 °C exhibit a high negative ZP of -20.6 mV. Compared to CNPs, cerium oxide microparticles (micrometer ceria) of size ~1–2 μm exhibit the highest negative ZP value of -29.0 mV. The gradual shift in ZP from positive to negative values of annealed CNPs and micrometer ceria can be correlated with the temperature dependent annealing of oxygen vacancy defects in cerium oxide. The lower concentration of oxygen vacancies in annealed CNPs would result in a reduced production of H<sub>3</sub>O<sup>+</sup> as the rate of H<sub>2</sub>O dissociation decreases. This reduces the rate of proton adsorption by CNPs and increases the rate of adsorption of more favorable OH<sup>-</sup> ions, resulting in a gradual increase in the magnitude of negative ZP with the annealing temperature.

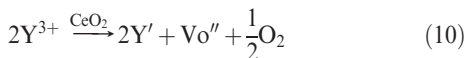
The ZP variations observed with CNPs annealed at different temperatures indicate that oxygen vacancies could play a major role in tuning the ZP of CNPs. It is well-known that by addition of trivalent dopants the concentration of oxygen vacancy in CNPs can be tuned to a great extent.<sup>45</sup> Depending on the size of these

(44) Lai, T.-Y.; Lee, W.-C. *J. Photochem. Photobiol. A: Chem.* **2009**, *204* (2–3), 148.

(45) Patil, S.; Seal, S.; Guo, Y.; Schulte, A.; Norwood, J. *Appl. Phys. Lett.* **2006**, *88*(24), 243110.

(46) Mamontov, E.; Egami, T.; Brezny, R.; Koranne, M.; Tyagi, S. *J. Phys. Chem. B* **2000**, *104*(47), 11110.

dopant cations, the oxygen vacancy concentration can be either increased or decreased. To understand the effect of doping on the ZP of CNPs, yttrium (Y) and ytterbium (Yb) were doped into CNPs. When Ce<sup>4+</sup> ions are substituted by large rare earth trivalent ions such as Y<sup>3+</sup>, the oxygen vacancies are created due to the partial reduction of Ce<sup>4+</sup> to Ce<sup>3+</sup>. The formation of oxygen vacancies can be represented as



where Vo'' is the oxygen vacancy concentration. Earlier, we reported that ceria contains  $\sim 3.39 \times 10^{20} \text{ cm}^{-3}$  oxygen vacancies and doping with larger ion such as Y<sup>3+</sup> can lead to an increase in the lattice parameter (0.0552% increase with 20% doping) and thus to an increase in the oxygen vacancy concentration (1.77% increase with 20% doping), whereas a decrease in lattice parameter (0.223% decrease with 20% doping) and oxygen vacancy concentration (7.97% decrease with 20% doping) was observed while doping with smaller ions like Yb<sup>3+</sup>.<sup>47</sup> The doped CNP solution was then heated at different temperatures, and their ZP variations with temperature were monitored (Figure 7b). Similar to the undoped CNPs, the magnitude of positive ZP of doped CNPs decreases with increase in temperature, and at 65 °C, the doped CNPs exhibits a negative ZP. At the temperatures below 50 °C, 20% yttrium-doped CNPs (Y-CNPs) exhibit the highest positive ZP while 20% ytterbium-doped CNPs (Yb-CNPs) exhibit the lowest ZP as compared to that of pure CNPs (pure-CNPs). The magnitude of ZP decreased in the same order, Y-CNPs > pure-CNPs > Yb-CNPs. This observation can be correlated with the oxygen vacancy defect concentration in these CNPs, which decrease in the same order Y-CNPs > pure-CNPs > Yb-CNPs.<sup>47</sup> The results directly indicate that CNPs with more oxygen vacancies engage in the dissociation of more number of H<sub>2</sub>O and undergo higher proton adsorption. Inconsistent trends in the data at 55 and 65 °C could be due to the difference in the reaction kinetics of pure and doped CNPs at that temperature range.

**Oxygen Vacancy Modulated Nanoceria–Proton Interactions.** To better understand the role of oxygen vacancies in determining the ZP of CNPs, DFT simulations were carried out by considering different levels of protonation varying from one to six H<sup>+</sup> ions on the surface of CNP. Figure 7c shows the BE profile of H<sup>+</sup> ions interacting with CNP as a function of H<sup>+</sup> ion added. The effective BE decreases with increase in the number of H<sup>+</sup> ions attached to the CNP surface, and additional protonation becomes thermodynamically unfavorable after the BE value passes through zero. After the oxygen vacancies are introduced into the CNP, the proton binding energy also decreases, whereas the zero BE value is reached after the addition of four protons (vs two for CNP without the vacancy). These data indicate that CNPs with higher concentration of the oxygen vacancies will associate with more H<sup>+</sup> ions and will have high positive ZP values. Similar trend is observed for Y-CNP. As one can see from Figure 7d, Y-CNP exhibits higher binding affinity toward H<sup>+</sup> ions as indicated by their high BE values and is capable to attach as many protons as CNP with one vacancy. These computational results explain why the pure CNPs display higher positive ZPs as compared to the annealed CNPs, and the doped CNPs display higher positive ZPs as compared to pure CNPs.

### Physicochemical Implications in Chemical Mechanical Planarization (CMP) Slurry.

Cerium oxide based slurries have

(47) Babu, S.; Thanneeru, R.; Inerbaev, T.; Day, R.; Masunov, A. E.; Schulte, A.; Seal, S. *Nanotechnology* **2009**, 20(8), 085713.

been used for glass polishing for several years.<sup>12</sup> Recently, the use of ceria slurries has been extended to chemical–mechanical polishing (CMP) processes<sup>48</sup> in the microelectronics industry such as those involving the fabrication of integrated circuit (IC) photomasks,<sup>49</sup> glasses for the liquid crystalline displays (LCD),<sup>50</sup> and interlayer dielectrics (ILDs).<sup>51</sup> The interaction of abrasive particle with the polishing surface has been a major focus of study in CMP.<sup>52,53</sup> Since the polishing process occurs in an aqueous environment (pH 7–10),<sup>52</sup> pH dependent charge modifications can occur on both ceria and silica glass surfaces. The literature reported value of PZC of silica is about 1.5–2.8.<sup>54</sup> Hence, silica exhibits a high negative ZP at pH  $\geq 7$ .<sup>52</sup> It is reported that the removal of material from the surface of silica glass during CMP polishing process is attributed to a temporary attachment of CNPs to the silica glass surface through surface chemical bonds.<sup>52</sup>

The surface charges of CNPs can influence the ceria–silica interaction and play a major role in the polishing process. In pH 7–10 range, CNPs can exhibit positive, neutral, or negative surface charge depending on the nature of NPs used for polishing. Our experimental observations display that freshly prepared CNPs (PZC  $\sim 10$ ) exhibit positive ZP values of +37.8, +22.7, and +5.68 mV when treated with pH 7–9 buffers and 0.00 mV when treated with pH 10 buffer. However, within 40–220 days of aging in water, the ZP of these CNPs switched to the negative ZP values of -30.7, -28.9, -36.0, and -32.0 mV. These negative charged CNPs could experience a strong repulsion from the negatively charged silica and could adversely affect the atomic scale polishing process. Hence, it is necessary to use freshly prepared CNPs rather than aged CNPs for the CMP process.

Figures 8a–d show the AFM-based force–displacement (F–D) spectroscopy data of a silica bead of size 600 nm interacting with freshly prepared (+43.0 mV ZP) and aged (-23.0 mV ZP) CNPs in water (negative charges on CNPs are obtained by natural aging process and not by any basic buffer treatment). It is clear that the adhesion force of silica bead with freshly prepared CNPs is much higher compared to aged CNPs. The force distribution shows that the peak interaction force between the silica bead and freshly prepared CNPs is in the range of 400–500 nN (with a maximum at 600 nN), while for aged CNPs, the peak interaction force is observed mostly between 0 and 20 nN (with a maximum at 140 nN). F–D spectroscopy data reveal that it is important to use freshly prepared CNPs for CMP slurry to achieve a better adhesion of the ceria abrasive particles with silica surface. The experimental observations from the CNP aging process indicate that the NPs could undergo charge reversal with time and temperature during CMP process especially in basic pH conditions. Hence, it is important to start with freshly prepared slurry of positively charged CNPs for CMP process. It is also essential to monitor the changes in the ZP to determine the shelf life of the slurry depending upon the storage time and especially operational temperatures.

### Biomedical Implications in Targeted Drug Delivery: Transferrin–Nanoceria Interactions.

Ligand–receptor mediated drug delivery and imaging systems have been a major

(48) Sabia, R.; Stevens, H. J. *Mach. Sci. Technol.* **2000**, 4(2), 235.

(49) Janoš, P.; Petrák, M. *J. Mater. Sci.* **1991**, 26(15), 4062.

(50) Dana, L. Z. *Ceram. Eng. Sci. Proc.* **2008**, 16, 302.

(51) Homma, Y.; Furusawa, T.; Morishima, H.; Sato, H. *Solid-State Electron.* **1997**, 41(7), 1005.

(52) Cook, L. M. *J. Non-Cryst. Solids* **1990**, 120(1–3), 152.

(53) Rajan, K.; Singh, R.; Adler, J.; Mahajan, U.; Rabinovich, Y.; Moudgil, B. M. *Thin Solid Films* **1997**, 308–309, 529.

(54) Parks, G. A. *Chem. Rev.* **1965**, 65(2), 177.

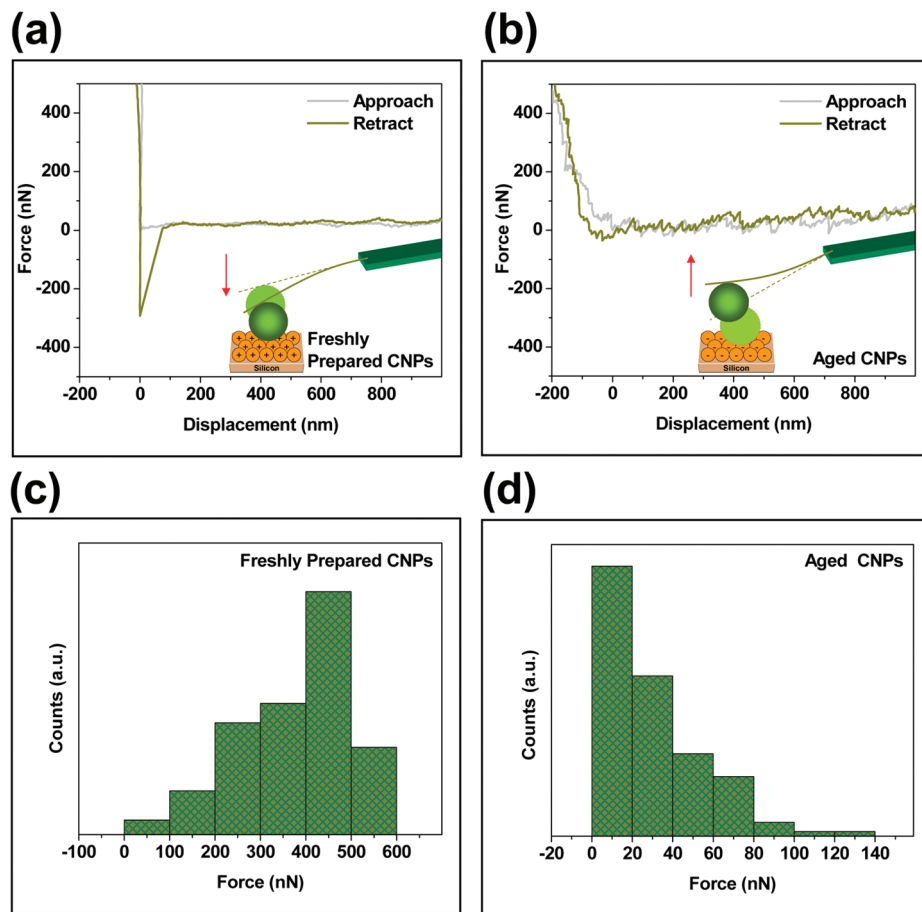


**Figure 8.** Force–displacement spectroscopy of 600 nm silica bead interacting with (a) freshly prepared (+43.0 mV ZP) CNPs and (b) aged (−23.0 mV ZP) CNPs. The corresponding force histograms are shown in (c) and (d). Force histograms are obtained by conducting multiple SMFS measurements on each sample. The total number of force values analyzed is  $n = 130$  in each case.

focus of study in nanomedicine.<sup>55,56</sup> NPs conjugated with cellular targeting proteins<sup>5,57,58</sup> (mostly anionic) and polymer transfection agents<sup>59,60</sup> (mostly cationic) are a topic of active biomedical research. This conjugation relies predominantly on the high surface area and surface charge of the NPs, leading to the Coulombic attachment.<sup>5,11</sup> Under physiological pH conditions, the ligands may exhibit positive or negative charges with respect to their PZC. Hence, depending on the nature of ligand molecules, NPs engineered with appropriate surface charges are often chosen to achieve better NP–ligand binding.<sup>11</sup>

Transferrin (Tf) is a protein used in biological systems for the transportation and supply of iron to the growing cells. It has been used as a targeting ligand to deliver a wide range of therapeutic agents including NPs to cells that overexpress transferrin receptor (TFRs).<sup>5,57,61–64</sup> In order to demonstrate the influence of ZP

changes with aging time on Tf–CNP interactions, single molecule force spectroscopy measurements were conducted on both freshly prepared and 220 days aged CNPs using Tf-coated AFM probes.

Figures 9a,b show the force spectroscopy of Tf-coated AFM probe (Figure 9c) interacting with freshly prepared (+43.0 mV ZP) and aged (−23.0 mV ZP) CNPs. It is clear from the figure that the Tf interacts strongly with freshly prepared CNPs while it experienced much less and mostly negligible interaction with aged CNPs. The unbinding forces obtained here in both the cases are similar to that observed in our earlier studies of Tf interaction with acidic/basic buffer treated surface charge tuned positive (+36.0 mV) and negative (−35.0 mV) CNPs.<sup>5</sup> Our experiments shows that Tf experienced a strong unbinding force of 100–400 pN with freshly prepared CNPs while it experienced an unbinding force of much less magnitude (0–75 pN) with aged CNPs. These observations suggests that it is essential to use freshly prepared positively charged CNPs for achieving better Tf–CNP conjugation to ensure a strong electrostatic attraction. CNPs dispersed in water can undergo charge reversal with time, and their ability to form bonds with Tf can deteriorate due to the strong columbic repulsion between the negatively charged CNPs and the negatively charged Tf.

## Summary

Surface charges of the NPs have implications not only on the dispersibility but also on many potential applications. The present experimental results along with theoretical calculations presented

- (55) Vyas, S. P.; Singh, A.; Sihorkar, V. *Crit. Rev. Ther. Drug Carrier Syst.* **2001**, 18(1), 1.
- (56) Gao, X.; Cui, Y.; Levenson, R. M.; Chung, L. W. K.; Nie, S. *Nat. Biotechnol.* **2004**, 22(8), 969.
- (57) Qian, Z. M.; Li, H.; Sun, H.; Ho, K. *Pharmacol. Rev.* **2002**, 54(4), 561.
- (58) Low, P. S.; Antony, A. C. *Adv. Drug Delivery Rev.* **2004**, 56(8), 1055.
- (59) Boussif, O.; Lezoualch'h, F.; Zanta, M. A.; Mergny, M. D.; Scherman, D.; Demeneix, B.; Behr, J. P. *Proc. Natl. Acad. Sci. U.S.A.* **1995**, 92(16), 7297.
- (60) Rosenholm, J. M.; Meinander, A.; Peuhu, E.; Niemi, R.; Eriksson, J. E.; Sahlgren, C.; Lindén, M. *ACS Nano* **2009**, 3(1), 197.
- (61) Iinuma, H.; Maruyama, K.; Okinaga, K.; Sasaki, K.; Sekine, T.; Ishida, O.; Ogiwara, N.; Johkura, K.; Yonemura, Y. *Int. J. Cancer* **2002**, 99(1), 130.
- (62) Ishida, O.; Maruyama, K.; Tanahashi, H.; Iwatsuru, M.; Sasaki, K.; Eriguchi, M.; Yanagie, H. *Pharm. Res.* **2001**, 18(7), 1042.
- (63) Yang, P.-H.; Sun, X.; Chiu, J.-F.; Sun, H.; He, Q.-Y. *Bioconjugate Chem.* **2005**, 16(3), 494.
- (64) Chithrani, B. D.; Chan, W. C. W. *Nano Lett.* **2007**, 7(6), 1542.

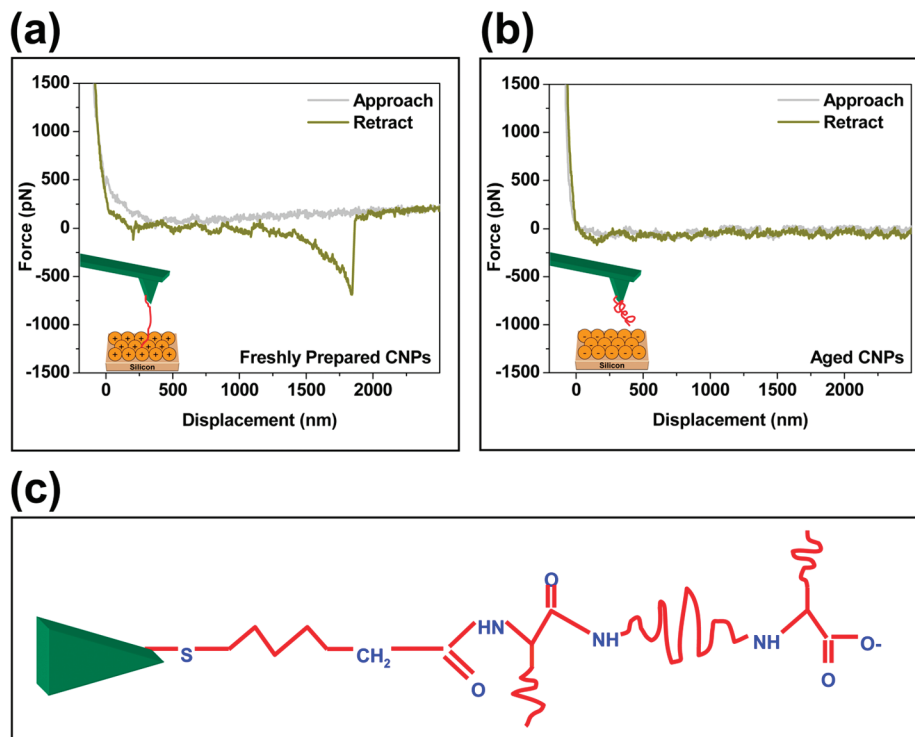


**Figure 9.** Single molecule force spectroscopy of Tf protein interacting with (a) freshly prepared (+43.0 mV ZP) CNPs and (b) aged (−23.0 mV ZP) CNPs. Freshly prepared CNPs exhibits higher binding affinity with Tf compared to aged CNPs. (c) Schematic diagram of transferrin conjugated AFM tip.

here demonstrate that CNPs, when dispersed in water, exhibit positive ZP due to a kinetically driven proton adsorption process. However, the initial positive ZP of CNPs is highly unstable, and prolonged exposure to water and/or increasing the solution temperature and/or lowering the CNP concentration, the CNPs undergo a ZP switch from positive to negative values by adsorbing OH<sup>−</sup> ions on the NP surface, resulting in thermodynamically stable state. Positively charged CNPs exhibit a better adhesion interaction with silica beads (chemical mechanical planarization applications) and a better ligand conjugation with cellular targeting transferrin protein (drug delivery applications), while negatively charged CNPs displayed negligible adhesion to both protein and silica beads. The data presented here demonstrate that the surface charges of CNPs play a vital role in their efficient use as a targeted drug delivery carrier in biomedical or as an abrasive material in CMP applications. In order to tailor the surface properties of colloidal NPs for intended applications, it is essential

to understand the dynamics of the physicochemical surface reactions occurring on the colloidal NP surface.

**Acknowledgment.** We thank the National Science Foundation (NIRT CBET 0708172) and National Institute of Health (R01: AG031529-01) for funding this work. This research used computational resources from (1) the National Energy Research Scientific Computing Center (NERSC), which is supported by the Office of Science of the U.S. Department of Energy under Contract DE-AC02-05CH11231; (2) IBM HPCC facility at the UCF Institute for Simulation and Training (IST); and (3) SGI Altix 350 SMP facility at the UCF NanoScience Technology Center (NSTC).

**Supporting Information Available:** HRTEM images of freshly prepared and aged CNPs (Figure S1). This material is available free of charge via the Internet at <http://pubs.acs.org>.